Available online at www.sciencedirect.com
SCIENCE DIRECT®
C. R. Chimie 9 (2006) 1014–1021
COMPTES RENDUS CHIMIE
http://france.elsevier.com/direct/CRAS2C/

Account / Revue

Photoinduced intermolecular electron transfer and energy transfer of C_{60} dendrimers

Yasuyuki Araki [a], Ryouta Kunieda [a], Mamoru Fujitsuka [a], Osamu Ito [a,*], Jiro Motoyoshiya [b], Hiroshi Aoyama [b], Yutaka Takaguchi [c]

[a] *Institute of Multidisciplinary Research for Advanced Materials, Tohoku University, Kaahira, Aoba-ku, Sendai 980-8577, Japan*
[b] *Faculty of Textile Science and Technology, Shinshu University, Ueda, Nagano 386-8567, Japan*
[c] *Graduate School of Natural Science and Technology, Okayama University, Tsushimanaka, Okayama 700-8530, Japan*

Received 1 July 2005; accepted after revision 24 August 2005
Available online 27 January 2006

Abstract

Photoinduced intermolecular electron-transfer and energy-transfer processes of the fullerodendrimers with two poly(amidoamine) dendron groups of 0.5-th, 1.5-th and 2.5-th generations have been investigated by laser flash photolysis. The rate constants and quantum yields of photoinduced electron transfer with the added aromatic amine donors in PhCN tend to decrease with the dendron generation, indicating that the bulky dendron groups act as barriers for the donor molecules to approach the C_{60} moiety in the center of the dendrimers. The decreases in the rate constants of triplet energy transfer processes vs. O_2 and β-carotene with the dendron generation are smaller than those of electron-transfer process, probably because effective encounter radii for energy transfer are larger than those for electron transfer; hence, less sensitive to dendrimer generation. A kinetic model for intermolecular electron-transfer and energy-transfer of fullerodendrimers was proposed. ***To cite this article: Yasuyuki Araki et al., C. R. Chimie 9 (2006)***.

Keywords: Fullerene; Dendrimer; Electron-transfer; Energy-transfer; Laser flash photolysis

Fullerene functionalized dendrimers have recently been studied extensively, because they are very interesting in structural and synthetic chemistry [1–4]. The studies on syntheses and properties of various fullerodendrimers have been reported, showing various possibilities to apply to the field of supramolecular chemistry and material science [1,5–12]. Fullerene-based dendrimers have been revealed to be effective for application to artificial photosynthesis systems [13–17]. In general, introduction of dendritic branches to fullerene can improve solubility and easy fabrication into nanoparticles [16,17] and films [18]. Furthermore, by the introduction of additional functionalities to the dendrons, these new fullerodendrimers have high possibilities to be widely applied as new materials. However, there are a few reports on photochemical and photoinduced intermolecular kinetics of fullerodendrimers [19–21]. It has been revealed in our previous report that photoinduced bimolecular processes such as photoinduced electron transfer are much affected by the dendron generation [22]. This feature was beneficial to control the reactivity of the unstable states of the fullerene core such as triplet ex-

* Corresponding author.
E-mail address: ito@tagen.tohoku.ac.jp (O. Ito).

1631-0748/$ - see front matter
doi:10.1016/j.crci.2005.09.008

cited state, radical anion, and anion of the C_{60} moiety. Therefore, it is interesting to reveal further the dendrimer effects on photochemical and photophysical properties of fullerodendrimers.

In the present study, we studied fullerodendrimers in which C_{60} is attached to poly(amidoamine)-type dendrons through the sulfide bonds as shown in Fig. 1; fullerodendrimers are represented as C_{60}–(GnB)$_2$ (n = 0.5, 1.5, and 2.5). For C_{60}–(GnB)$_2$, since the dendron groups do not contain aromatic rings, it is expected that the dendron groups are very flexible covering the C_{60} core.

Photoinduced electron transfer of the fullerodendrimers with the aromatic amine donors such as *N,N′*-tetramethylbenzidine (TMB) and *N,N′*-tetramethyl-*p*-phenylenediamine (TMPD) was investigated to disclose the dendrimer effects on bimolecular electron transfer processes. As for energy transfer, the triplet energy transfer from the fullerodendrimers to O_2 and β-carotene has been studied. For these investigations, nanosecond laser flash photolysis techniques measuring the near-IR transient absorption spectra have been effectively used to follow the kinetic behavior of the triplet states of the fullerenes [23].

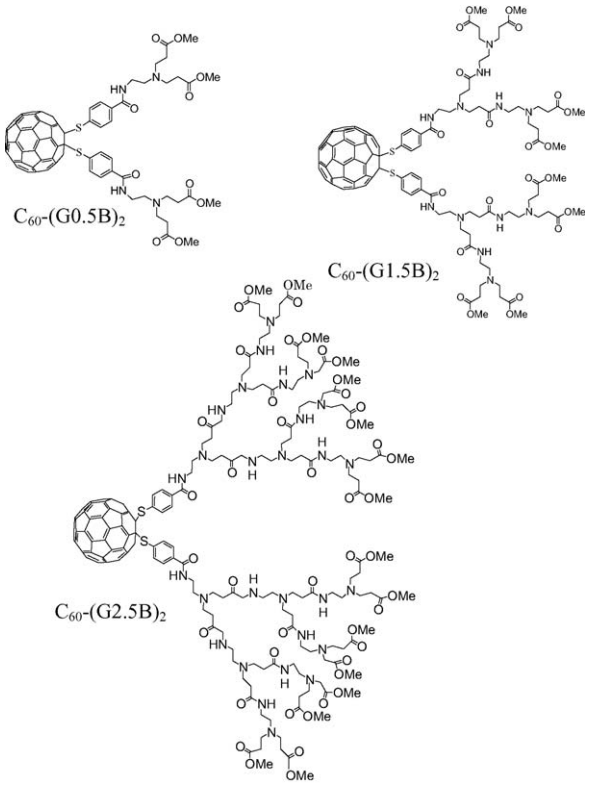

Fig. 1. Molecular structures.

Fullerodendrimers, C_{60}–(GnB)$_2$ (n = 0.5, 1.5, 2.5), were prepared by the photochemical reactions between C_{60} and five equivalent disulfide derivatives of the dendron group under photoirradiation (> 300 nm) in the presence of five equivalent diphenyldiselenide in dichloromethane [12].

Optimized molecular structures of C_{60}–(GnB)$_2$ were calculated by the molecular dynamics at 300 K by using OPSL-AA force field in the MacroModel package [24]. In general, molecular dynamics using the OPSL-AA force field gave the fluctuation among the possible molecular structures with flexible substituents. Thus, in Fig. 2 (left side), each typical structure selected among the possible molecular structures found in the calculation is depicted for each fullerodendrimer. In C_{60}–(G0.5B)$_2$, most part of C_{60} moiety is exposed from the dendron extending in one direction. For C_{60}–(G1.5B)$_2$, the C_{60} moiety is appreciably exposed from the dendrons, which covers the C_{60} moiety as an umbrella. In C_{60}–(G2.5B)$_2$, the C_{60} moiety is almost

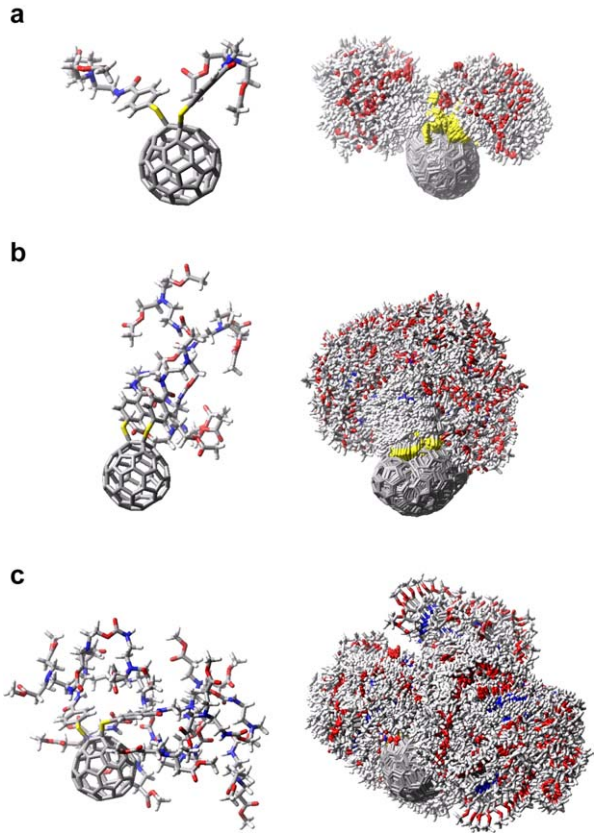

Fig. 2. Left: Typical structures of (**a**) C_{60}–(G0.5B)$_2$, (**b**) C_{60}–(G1.5B)$_2$, and (**c**) C_{60}–(G2.5B)$_2$ founded in molecular dynamics calculation at 300 K by using OPSL-AA force field. Right: Superposition of 200 optimized structures of C_{60} dendrimers by molecular dynamics calculation.

covered with the dendron and the exposed part of the C_{60} moiety is quite small. By the fluctuations with time at room temperature, the exposed parts of the C_{60} moiety are further decreased as shown in Fig. 2 (right side), in which 200 structures are superimposed keeping the gravity of the C_{60} moiety at the same position. These fluctuated structures also suggested that the radii of C_{60}–(GnB)$_2$ increase with the generation of dendron group. The maximal radii (R_{total}) from the center of the C_{60} moiety to the edge of the dendron were evaluated to be 1.5, 1.8, and 2.1 nm for C_{60}–(G0.5B)$_2$, C_{60}–(G1.5B)$_2$, and C_{60}–(G2.5B)$_2$, respectively, from Fig. 2.

Fig. 3a shows the transient absorption spectra observed by the excitation of C_{60}–(G1.5B)$_2$ with the laser light at 532 nm in the presence of TMPD in toluene. The transient absorption bands at 600, 730, and 1050 nm are attributed to TMPD$^{\bullet+}$, $^3C_{60}$*–(G1.5B)$_2$, and $C_{60}^{\bullet-}$–(G1.5B)$_2$, respectively [25–30]. The absorption intensities of the bands at 600 and 1050 nm increased with concomitant decay of the band at 730 nm (inset of Fig. 3a). This observation indicates that the radical ions are generated by the electron transfer via $^3C_{60}$*–(G1.5B)$_2$. The same phenomena were also confirmed for other dendrimers and donors in toluene. Thus, the electron transfer process is described as Eq. 1, in which the radical ion–pair states between $C_{60}^{\bullet-}$–(GnB)$_2$ and Amine$^{\bullet+}$ may depend on the solvent polarity and size of dendrimers:

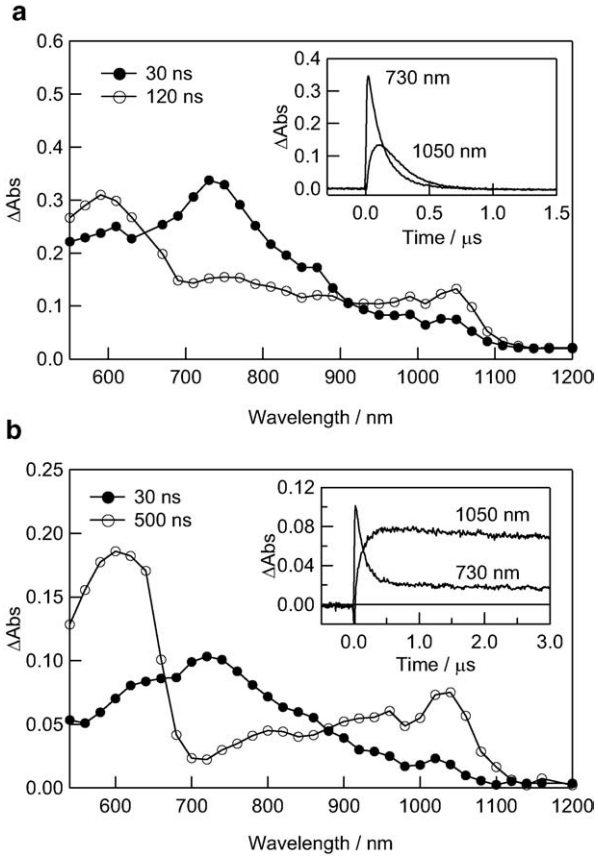

Fig. 3. Transient absorption spectra C_{60}–(G1.5B)$_2$ (0.1 mM) observed by excitation with 532 nm laser light in the presence of TMPD (2.0 mM) in (**a**) toluene and (**b**) PhCN. Inset: Absorbance-time profiles.

$$^3C_{60}^{*}-(GnB)_2 + \text{Amine} \xrightarrow{k_{ET}(\text{amine})} C_{60}^{\bullet-} - (GnB)_2 + \text{Amine}^{\bullet+} \quad (1)$$

In toluene, after reaching a maximum, the generated $C_{60}^{\bullet-}$–(G1.5B)$_2$ begins to decay within 0.6 μs. Compared with time profiles of the pristine $C_{60}^{\bullet-}$ and $^3C_{60}$* in toluene [26] in which $C_{60}^{\bullet-}$ decayed within 0.1 μs because $C_{60}^{\bullet-}$ forms the contact ion-pair with Amine$^{\bullet+}$, the observed rise and decay of $C_{60}^{\bullet-}$–(G1.5B)$_2$ and $^3C_{60}$*–(G1.5B)$_2$ were quite slow (Fig. 3a). Thus, the bulky dendrimers may separate the radical ion–pairs, slowing down the decay of $C_{60}^{\bullet-}$–(G1.5B)$_2$. Thus, this is one of the characteristics of the dendrimers electron-transfer systems; that is, the radical ions are present as looser radical ion-pair even in nonpolar toluene, whereas contact radical ion-pairs are present for pristine $C_{60}^{\bullet-}$ in toluene [25,26].

In PhCN (Fig. 3b), quick rise of $C_{60}^{\bullet-}$–(G1.5B) was observed with the decay of $^3C_{60}$*–(G1.5B)$_2$, although the decay of $C_{60}^{\bullet-}$–(G1.5B)$_2$ was slower than that in toluene. In PhCN, only 10% of $C_{60}^{\bullet-}$–(G1.5B)$_2$ decayed during 3 μs, suggesting that $C_{60}^{\bullet-}$–(G0.5B)$_2$ and TMPD$^{\bullet+}$ are separately solvated in PhCN behaving as free radical ions, which need time to encounter longer than 100 μs in the rate of a diffusion controlled limit in PhCN under their low concentrations.

From the pseudo-first-order relation between the decay rates of $^3C_{60}$*–(GnB)$_2$ and the excess concentrations of aromatic amine donors, the bimolecular quenching rate constants (k_q(amine)) were estimated as summarized in Table 1 (PhCN). In toluene, the k_q(amine) values are in the region of (1–3) × 10^9 s^{-1}; the variation with the dendrimer generation was quite small.

The quantum yield of electron transfer (Φ_{ET}(amine)) via $^3C_{60}$*–(GnB)$_2$ can be evaluated from the ratio of the maximal concentration of $C_{60}^{\bullet-}$–(GnB)$_2$ to the initial concentration of $^3C_{60}$*–(GnB)$_2$ at the amine concentrations higher than 1.0 mM (Fig. 4). Thus, the k_{ET}(amine) values were estimated by the relation of k_{ET}(amine) = Φ_{ET}(amine) × k_q(amine). These values for TMB and TMPD are listed in Table 1. In toluene, appreciable changes were not observed for the Φ_{ET}(amine) values.

In PhCN, the k_q(amine) values tend to decrease with an increase in the dendron generation of C_{60}–(GnB)$_2$

Table 1
Quenching rate constants (k_q(amine)), quantum yields (Φ_{ET}(amine)), rate-constants (k_{ET}(amine)) of electron-transfer processes between $^3C_{60}$*–(G*n*B)$_2$ and amines, and back electron-transfer rate-constants (k_{BET}^{2nd}) in PhCN

C_{60}–(G*n*B)$_2$	Amines	k_q(amine) (M^{-1} s^{-1})	Φ_{ET}(amine)	k_{ET}(amine) (M^{-1} s^{-1})	k_{BET}^{2nd}/M^{-1} s^{-1}
C_{60}–(G0.5B)$_2$	TMB	6.6×10^9	1.00	6.6×10^9	4.6×10^9
C_{60}–(G0.5B)$_2$	TMPD	3.7×10^9	0.80	3.0×10^9	19×10^9
C_{60}–(G1.5B)$_2$	TMB	3.5×10^9	0.79	2.8×10^9	4.3×10^9
C_{60}–(G1.5B)$_2$	TMPD	2.5×10^9	0.60	1.5×10^9	15×10^9
C_{60}–(G2.5B)$_2$	TMB	1.6×10^9	0.85	1.4×10^9	3.8×10^9
C_{60}–(G2.5B)$_2$	TMPD	1.4×10^9	0.68	9.5×10^8	30×10^9

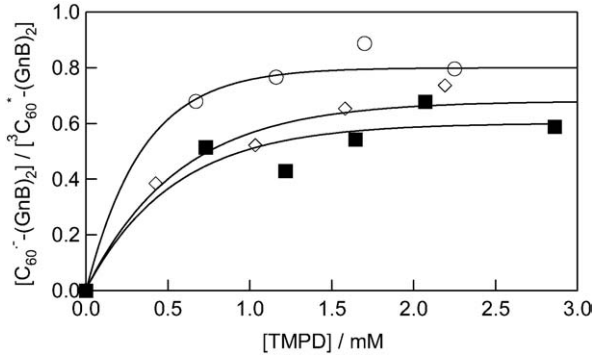

Fig. 4. Relations between [$C_{60}^{\bullet-}$–(GnB)$_2$]/[$^3C_{60}$*–(G*n*B)$_2$] values and concentrations of TMPD in PhCN. (○): C_{60}–(G0.5B)$_2$, (■): C_{60}–(G1.5B)$_2$, (◊): C_{60}–(G2.5B)$_2$, respectively.

(Table 1 and Fig. 5), indicating that the dendron groups prevent the amine molecules from approaching to the C_{60} core, acting as a barrier [22]. For aromatic amines such as TMB and TMPD, the Φ_{ET}(amine) values of $^3C_{60}$*–(G2.5B)$_2$ are larger than those of $^3C_{60}$*–(G1.5B)$_2$, suggesting that the dendrons spreading widely act as nets catching the donor molecules. Finally, the k_{ET}(amine) values tend to decrease monotonously with the dendrimer generation as shown in Fig. 5.

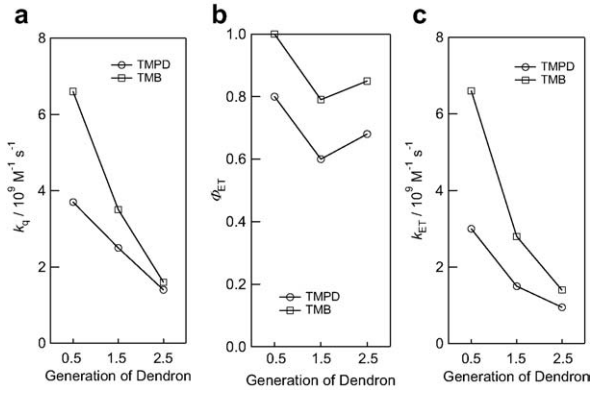

Fig. 5. Variations with dendron generation of (**a**) k_q, (**b**) Φ_{ET}, and (**c**) k_E for aromatic amines in PhCN.

Since the oxidation potential of TMB is lower than that of TMPD in polar solvents [31], the electron-donor ability of TMB is expected to be higher than that of TMPD. In each $^3C_{60}$*–(GnB)$_2$, the k_q(amine), Φ_{ET}(amine), and k_{ET}(amine) values obey this order in PhCN.

After the photoinduced electron transfer, back electron transfer occurs as shown in time profiles in Fig. 6. For $C_{60}^{\bullet-}$–(G*n*B)$_2$ and TMPD$^{\bullet+}$ in toluene, the decay of the radical ions obeyed first-order kinetics within 0.2 μs (Fig. 6a), indicating that the radical ions are present as contact ion-pairs (Eq. 2):

$$(C_{60}^{\bullet-}-(GnB)_2, \text{Amine}^{\bullet+})_{\text{ion pair}} \xrightarrow{k_{BET}^{1st}} C_{60}-(GnB)_2 + \text{Amine} \quad (2)$$

On the other hand, in the case of the radical ions of $C_{60}^{\bullet-}$–(G2.5B)$_2$ and TMB$^{\bullet+}$ in toluene, the decay time-profile can be curve-fitted with bi-exponential functions (Fig. 6b), indicating that two kinds of the radical ion-pairs are present; one may be contact radical ion-pair and the other may be loose radical ion-pair. The variation of the k_{BET}^{1st} values for contact radical ion-pair with dendrimer generation was quite small, probably because the back electron transfer taking place within the oppositely charged species within the contact ion-pairs may not be affected by the size of the dendrons.

In PhCN, the decays of $C_{60}^{\bullet-}$–(G*n*B)$_2$ and Amine$^{\bullet+}$ obey second-order kinetics, indicating that the back electron transfer takes place after the radical ions were solvated as free ions (Eq. 3):

$$(C_{60}^{\bullet-}-(GnB)_2)_{\text{solv}}+(\text{Amine}^{\bullet+})_{\text{solv}} \xrightarrow{k_{BET}^{2nd}} C_{60}-(GnB)_2 + \text{Amine} \quad (3)$$

The second-order rate constants (k_{BET}^{2nd}) were evaluated as ratio of the ε values of the absorption bands of the radical ions; by employing the reported ε values [28,32,33], the k_{BET}^{2nd} values were calculated as listed in Table 1. Although the evaluated k_{BET}^{2nd} values for the systems of C_{60}–(G*n*B)$_2$ and TMB in PhCN are

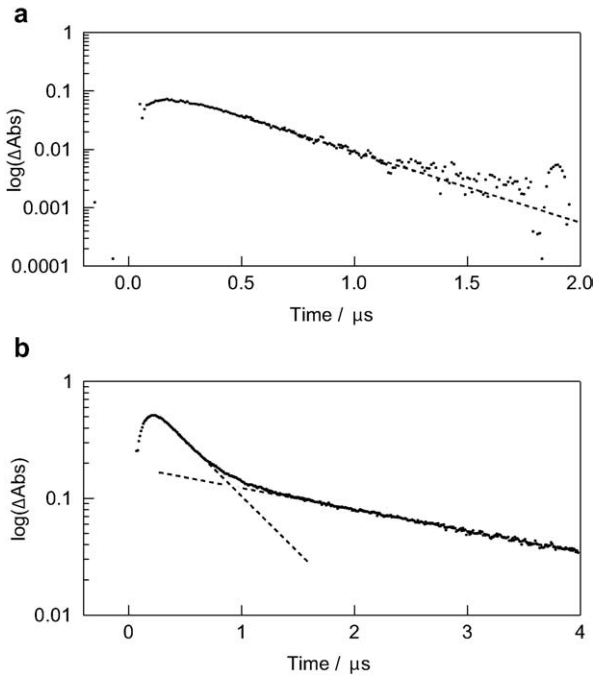

Fig. 6. First-order plots of absorption time profiles at 1030 nm of C_{60}^{-}–(G2.5B)$_2$ for (**a**) $TMPD^{\bullet+}$ and (**b**) $TMB^{\bullet+}$ in toluene.

smaller than those for TMPD, the dendrimer generation effect is small. The back electron transfer between the oppositely charged species may occur in the long-range over the dendrons. Furthermore, the oppositely charge species are possible to encounter with high directivity, avoiding the dendrons.

In the presence of O_2, $^3C_{60}$*–(G*n*B)$_2$ was quenched very fast; $^1O_2$* would be expected to be generated as Eq. 4 in nonpolar solvents, whereas electron transfer also contributes to the quenching of $^3C_{60}$*–(G*n*B)$_2$ in polar solvents (Eq. 5):

$$^3C_{60}\text{-(G}n\text{B)}_2\text{*} + {}^3O_2 \xrightarrow{\Phi_{O2}} C_{60}\text{-(G}n\text{B)}_2 + {}^1O_2\text{*} \quad (4)$$

$$^3C_{60}\text{-(G}n\text{B)}_2\text{*} + {}^3O_2 \xrightarrow{1-\Phi_{O2}} C_{60}\text{-(G}n\text{B)}_2{}^{\bullet+} + O_2{}^{\bullet-} \quad (5)$$

The bimolecular quenching rate-constants in the presence of O_2 ($k_q(O_2)$) were estimated from a pseudo-first-order relation between the decay rates of $^3C_{60}$*–(G*n*B)$_2$ and the O_2 concentrations, as listed in Table 2. The $k_q(O_2)$ values in toluene are larger than the corresponding values in PhCN. In each solvent, the $k_q(O_2)$ values are almost the same even by changing the dendron generation, indicating that approach of small O_2 molecule to the C_{60} moiety is not practically hindered by the dendron. The quantum yields for the production of $^1O_2$* (Φ_{O_2}) were determined by the comparison of

Table 2
Rate constants ($k_q(O_2)$) and quantum yields (Φ_{O2}) of energy transfer between $^3C_{60}$*–(G*n*B)$_2$ and O_2

C_{60}–(G*n*B)$_2$	Solvent	$k_q(O_2)$ (M^{-1} s^{-1})	Φ_{O_2}	$k_{EN}(O_2)$ (M^{-1} s^{-1})
C_{60}–(G0.5B)$_2$	Toluene	1.8×10^9	0.99	1.8×10^8
C_{60}–(G0.5B)$_2$	PhCN	1.3×10^9	0.77	1.0×10^9
C_{60}–(G1.5B)$_2$	Toluene	1.7×10^9	0.90	1.5×10^8
C_{60}–(G1.5B)$_2$	PhCN	1.2×10^9	0.75	0.9×10^9
C_{60}–(G2.5B)$_2$	Toluene	1.7×10^9	0.80	1.4×10^8
C_{60}–(G2.5B)$_2$	PhCN	1.2×10^9	0.63	0.8×10^9

Estimation error in each rate constant is ± 5%.

the $^1O_2$* emission with that of the pristine C_{60} as a standard (Fig. 7). The Φ_{O_2} values in PhCN are smaller than those in toluene, indicating that $^3C_{60}$*–(G*n*B)$_2$ was partly quenched by the electron-transfer process competitive with the energy-transfer process (Eq. 4). Total quantum yields of energy-transfer and electron-transfer processes are probably constant irrespective of the dendrimer generation for small O_2 molecule. With increas-

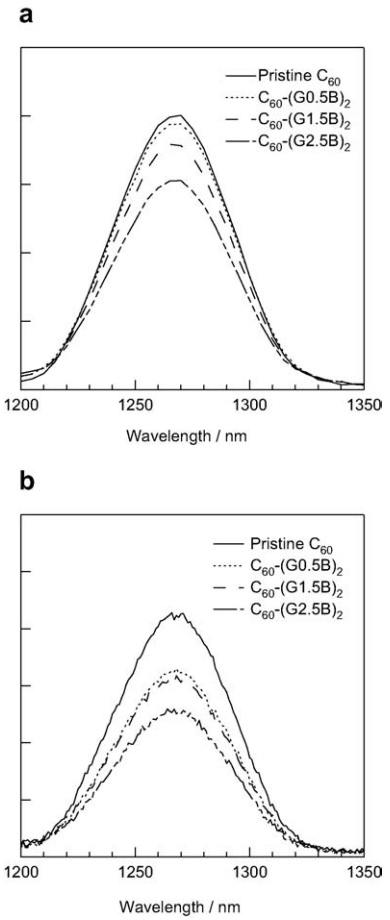

Fig. 7. $^1O_2$* emission spectra obtained by 514-nm laser irradiation to pristine C_{60} and C_{60}–(G*n*B)$_2$ (0.1 mM) in (**a**) toluene and (**b**) PhCN. Absorption intensity at 514 nm was matched in each sample.

ing the dendrimer generation, the Φ_{O_2} values decrease causing slight decrease in the $k_{EN}(O_2)$ values, which were obtained by $k_q(O_2) \times \Phi_{O_2}$ as listed in Table 2. Dendrimer generation-dependences of both Φ_{O_2} and $k_{EN}(O_2)$ values are smaller than those for electron transfer, indicating that the energy-transfer process is not much affected by the dendron crowding.

$^3C_{60}$*–(GnB)$_2$ was also quenched by β-carotene as transient absorption spectra and time profiles for $^3C_{60}$*–(G1.5B)$_2$, shown as an example in Fig. 8. With the decay of $^3C_{60}$*–(G1.5B)$_2$ at 700 nm, the characteristic absorption band of ^{3}β-carotene* increased at 520 nm. These transient absorption spectra and inserted time profiles indicate the energy transfer process from $^3C_{60}$*–(GnB)$_2$ to β-carotene as shown in Eq. 6:

$$^3C_{60}^*-(GnB)_2 + \beta-\text{Carotene} \xrightarrow{k_{ENT}(\beta-\text{carotene})} C_{60}-(GnB)_2 + {}^3\beta-\text{Carotene}* \quad (6)$$

The bimolecular triplet-energy quenching rate-constants in the presence of β-carotene (k_q(β-carotene)) were estimated from a psuedo-first-order relation between the decay rates of $^3C_{60}$*–(GnB)$_2$ and the β-carotene concentrations to be (1.7–2.9) × 10^8 M^{-1} s^{-1} as listed in Table 3. In both toluene and PhCN, the k_q(β-carotene) values tend to decrease on going from $^3C_{60}$*–(G0.5B)$_2$ to $^3C_{60}$*–(G1.5B)$_2$, while the change was not appreciable from $^3C_{60}$*–(G1.5B)$_2$ to $^3C_{60}$*–(G2.5B)$_2$. In PhCN, photoinduced electron transfer between $^3C_{60}$*–(GnB)$_2$ and β-carotene occurs simultaneously with energy transfer as reported in our previous report for pristine C_{60} and β-carotene, since the radical cation of β-carotene (β-carotene$^{\bullet+}$) appeared at 960 nm in addition to the radical anion of C_{60} ($C_{60}^{\bullet-}$) in the transient absorption spectra [34]. The variation of the k_q(β-carotene) values with the dendrimer generation is larger than that of the $k_q(O_2)$ values, probably because of the larger molecular size of β-carotene than that of O_2.

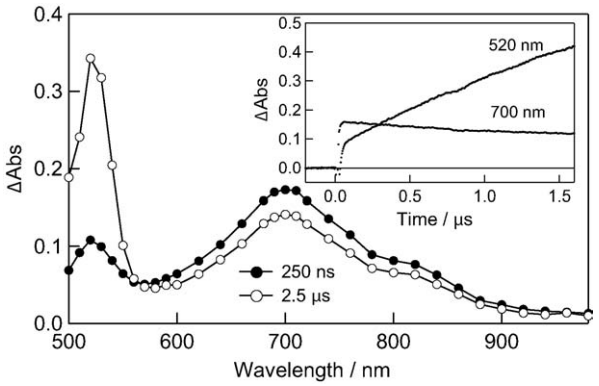

Fig. 8. Transient absorption spectra of C_{60}–(G1.5B)$_2$ (0.05 mM) observed by excitation with 532 nm laser light in the presence of β-carotene (1.0 mM) in toluene. Inset: Absorbance-time profiles at 520 and 700 nm.

Table 3
Rate constants k_q(β-carotene), and k_{ENT}(β-carotene)) and quantum yields ($\Phi_{ENT\ (\beta\text{-carotene})}$) of energy transfer between $^3C_{60}$*–(GnB)$_2$ and β-carotene

C_{60}–(GnB)$_2$	Solvent	k_q(β-carotene) (M^{-1} s^{-1})	Φ_{ENT} (β-carotene)	k_{ENT} (β-carotene) (M^{-1} s^{-1})
C_{60}–(G0.5B)$_2$	Toluene	2.9×10^8	(100)	2.9×10^8
C_{60}–(G0.5B)$_2$	PhCN	2.4×10^8	0.80	2.0×10^8
C_{60}–(G1.5B)$_2$	Toluene	2.0×10^8	(100)	2.0×10^8
C_{60}–(G1.5B)$_2$	PhCN	1.8×10^8	0.84	1.5×10^8
C_{60}–(G2.5B)$_2$	Toluene	1.9×10^8	(100)	1.9×10^8
C_{60}–(G2.5B)$_2$	PhCN	1.7×10^8	0.86	1.4×10^8

Estimation error in each rate constant is ± 5%.

The quantum yields of electron transfer from $^3C_{60}$*–(GnB)$_2$ to β-carotene (Φ_{ET}(β-carotene)) were evaluated from the ratio of β-carotene$^{\bullet+}$ to $^3C_{60}$*–(GnB)$_2$, as listed in Table 3, by employing the observed transient absorption intensities and reported ε values [34]. In PhCN, the Φ_{ENT}(β-carotene) values, which are equal to (1 – Φ_{ET}(β-carotene)) [34], increase slightly with the dendrimer generation. Then, the rate constants for energy transfer (k_{ENT}(β-carotene)), which can be evaluated by Eq. 7, decrease with the dendrimer generation, although the change between $^3C_{60}$*–(G1.5B)$_2$ and $^3C_{60}$*–(G2.5B)$_2$ is small.

$$k_{ENT}(\beta-\text{carotene}) = \Phi_{ENT}(\beta-\text{carotene}) \times k_q(\beta-\text{carotene}) \quad (7)$$

When energy transfer is predominant, the variation of the observed k_q(β-carotene) values with the dendrimer generation is smaller than that of the k_q(amine) values in PhCN. These trends suggest that energy transfer may be carried out not only by the collision with short distance (Dexter mechanism) [35], but also by the long collisional radii with the dipolar interaction (Förster mechanism) [36].

As a first approximation, the quenching rate constants (k_q^{pred1}) of $^3C_{60}$*–(GnB)$_2$ by the encounters with molecules can be thought to be proportional to the frequency factor (Z) as represented by Eq. 8 [21];

$$k_q^{pred1} \propto Z \approx \sigma \mu^{-1/2} \quad (8)$$

where σ refers to the cross-section proportional to the square of the radius of $^3C_{60}$*–(GnB)$_2$ ($\sigma \propto R_{total}^2$) and μ

refers to the reduced mass. From molecular dynamic calculations, the ratio of the R_{total} values for $^3C_{60}$*–(GnB)$_2$ was roughly estimated as 1:1.2:1.4 for n = 0.5:1.5:2.5. The ratio of $\mu^{1/2}$ was calculated to be 1:1.02:1.03 for the system of $^3C_{60}$*–(GnB)$_2$ and TMPD. Therefore, the ratio of the k_q^{pred1} values for $^3C_{60}$*–(G0.5B)$_2$: $^3C_{60}$*–(G1.5B)$_2$: $^3C_{60}$*–(G2.5B)$_2$ was evaluated to be 1.00:1.41:1.90. However, this ratio evaluated from Eq. 8 cannot reproduce the observed decreasing trend of the k_q values for $^3C_{60}$*–(GnB)$_2$ and TMPD with the dendrimer generation. Therefore, it is necessary to introduce calibration factor (f) by fitting the calculated k_q^{pred1} values with the observed k_q(amine) as shown in Fig. 9(a); the f values can be evaluated to be 1:0.48:0.20 for $^3C_{60}$*–(G0.5B)$_2$: $^3C_{60}$*–(G1.5B)$_2$: $^3C_{60}$*–(G2.5B)$_2$. The f values may be explained by the exposed volume of C_{60} (V_{C60}) from the dendrons. The shielding volumes of the dendrons, V_{shield}, can be roughly estimated by the cubic of the exclusive distance R_e (= R_{total} – R_{C60}) as defined in Fig. 10. The ratio, V_{C60}/V_{shield}, was calculated to be 1:0.49:0.27 for $^3C_{60}$*–(G0.5B)$_2$: $^3C_{60}$*–(G1.5B)$_2$: $^3C_{60}$*–(G2.5B)$_2$, which are in good agreement with the f values evaluated from Fig. 9a. Comparing two ratios, the ratio of V_{C60} can be evaluated to be 1.0:0.98:0.74 for $^3C_{60}$*–(G0.5B)$_2$:$^3C_{60}$*–(G1.5B)$_2$: $^3C_{60}$*–(G2.5B)$_2$, which seems to match with the MD result shown in Fig. 2.

By using the f values, we can predict the quenching rate constants of $^3C_{60}$*–(GnB)$_2$ with other electron donors and energy acceptors by the k_q^{pred2} values defined by Eq. 9:

$$k_q^{pred2} \propto k_q^{pred1} \times f \quad (9)$$

For electron transfer with TMB, quite good agreement was obtained between the k_q^{pred2} values and the observed k_q(TMB) values. For energy-transfer process, the results are shown in Fig. 9b and c. The ratios of the k_q^{pred2} values were not fitted well to those of the ob-

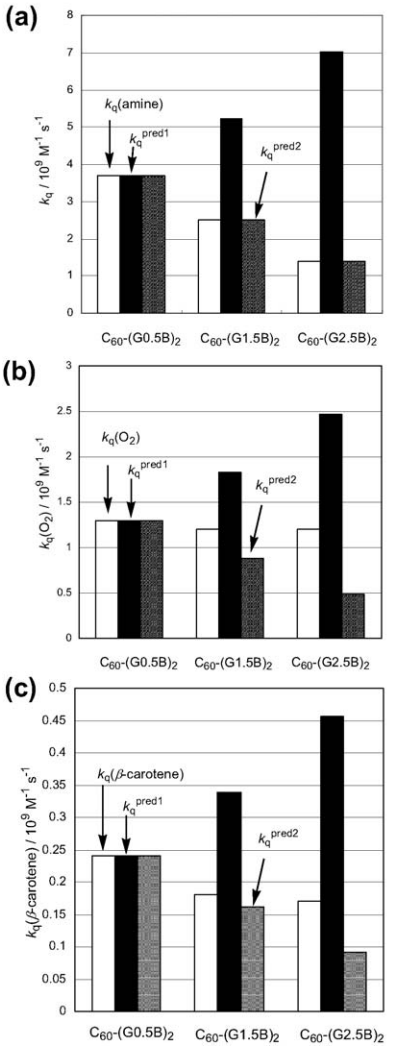

Fig. 9. Relative reactivities for (**a**) k_q(TMPD), (**b**) k_q(O_2), and (**c**) k_q(β-carotene) in PhCN.

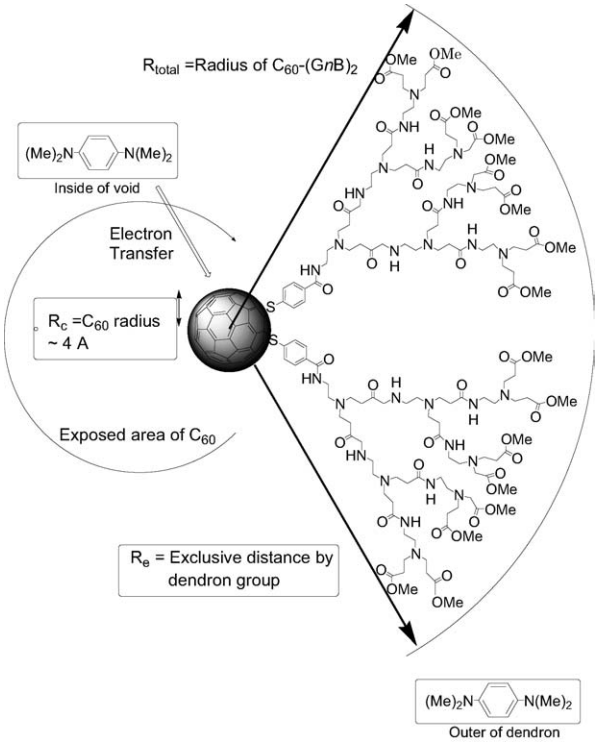

Fig. 10. Definition of radii and exclusive distance.

served $k_q(O_2)$ and k_q(β-carotene) values, which may be caused by the difference between the effective encounter radii of the electron-transfer process and the energy-transfer process. As mentioned before, the energy transfer from $^3C_{60}$*–(G*n*B)$_2$ to O_2 or β-carotene may be induced by not only Dexter mechanism, but also Förster mechanism. In the latter case, energy donor and acceptor are not necessary to counter each other, resulting in the inconsistency of the k_q^{pred2} due to the slight decrease in the ratio of the *f* values.

As conclusion, we revealed dendrimer generation effect on the photoinduced processes of the triplet states of fullerodendrimers, C_{60}–(G*n*B)$_2$ ($n = 0.5$, 1.5, and 2.5) by the nanosecond laser flash photolysis observing the transient absorption spectra in the visible and near-IR regions. Bimolecular processes such as electron transfer and energy transfer were affected by the dendron generation. In most cases, the bulky dendrons act as barrier for the reactant to approach the C_{60} core in fullerodendrimers. Sometimes, the dendrons act as net catching the donor molecules. From these kinetic data, the models for the bimolecular reactions of fullerodendrimers and reactants are proposed.

Acknowledgements

The authors are grateful to a financial support by a Grant-in-Aid on Scientific Research for Priority Aria (417) from the Ministry of Education, Culture, Sports, and Science.

References

[1] J.-F. Nierengarten, Chem.: Eur. J. 6 (2000) 3667.
[2] M.G. Nava, S. Setayesh, A. Rameau, P. Masson, J.-F. Nierengarten, New J. Chem. 26 (2002) 1584.
[3] J.-F. Nierengarten, N. Armaroli, G. Accorsi, Y. Rio, J.-F. Eckert, Chem.: Eur. J. 9 (2003) 36.
[4] M. Gutierrez-Nava, G. Accorsi, P. Masson, N. Armaroli, J.-F. Nierengarten, Chem.: Eur. J. 10 (2004) 5076.
[5] B. Dardel, D. Gullion, B. Heinrich, R. Deschenaux, J. Mater. Chem. 11 (2001) 2814.
[6] J.-F. Eckert, J.-F. Nicoud, J.-F. Nierengarten, J. Am. Chem. Soc. 122 (2000) 7467.
[7] C.J. Hawker, K.L. Wooley, M.J. Fréchet, J. Chem. Soc., Chem. Commun. 8 (1994) 925.
[8] A. Herzog, A. Hirsch, O. Vostrowsky, Eur. J. Org. Chem. 1 (2000) 171.
[9] F. Diederich, R. Kessinger, Acc. Chem. Res. 32 (1999) 537.
[10] J.-F. Nierengarten, J.-F. Eckert, Y. Rio, M.P. Carreon, J.-L. Gallani, D. Guillon, J. Am. Chem. Soc. 123 (2001) 9743.
[11] M. Schwell, N.K. Wachter, J.H. Rice, J.-P. Galaup, S. Leach, R. Taylor, R.V. Bensasson, Chem. Phys. Lett. 339 (2001) 29.
[12] Y. Takaguchi, K. Saito, S. Suzuki, K. Hamada, K. Ohta, J. Motoyoshiya, H. Aoyama, Bull. Chem. Soc. Jpn 75 (2002) 1347.
[13] D. Kuciauskas, P.A. Liddell, S. Lin, S.G. Stone, A.L. Moore, T.A. Moore, D. Gust, J. Phys. Chem. B 104 (2000) 4307.
[14] D.M. Guldi, A. Swatz, C. Luo, R. Gomez, J.L. Segura, N. Martín, J. Am. Chem. Soc. 124 (2002) 10875.
[15] M.-S. Choi, T. Aida, H. Luo, Y. Araki, O. Ito, Angew. Chem., Int. Ed. Engl. 42 (2003) 4060.
[16] T. Sasabe, P.V. Kamat, M.A. Absalom, Y. Kashiwagi, J. Sly, M.J. Crossley, K. Hosozumi, H. Imahori, S. Fukuzumu, J. Phys. Chem. B 108 (2004) 12865.
[17] T. Hasobe, P.V. Kamat, V. Troiani, N. Solladie, T.-K. Kim, S.-K. Kim, D. Kim, A. Kongkanand, S. Kuwabata, S. Fukuzumi, J. Phys. Chem. B 109 (2005) 19.
[18] C. Hirano, T. Imae, S. Fujima, Y. Yanagimoto, Y. Takaguchi, Langmuir 21 (2005) 272.
[19] I. Texier, M.N. Berberan-Santos, A. Ferorov, M. Brettreich, H. Schonberger, A. Hirsch, S. Leach, E. Bensasson, J. Phys. Chem. A 105 (2001) 10278.
[20] M. Martin, S. Atalick, D.M. Guldi, H. Lanig, M. Brettreich, S. Burghardt, M. Hatzimarinaki, E. Racvanelli, M. Prato, R. van Eldik, A. Hirsch, Chem. Eur. J. 9 (2003) 3867.
[21] X. Luo, M.-S. Choi, Y. Araki, O. Ito, T. Aida, Bull. Chem. Soc. Jpn 78 (2005) 371.
[22] R. Kunieda, M. Fujitsuka, O. Ito, M. Ito, Y. Murata, K. Komatsu, J. Phys. Chem. B 106 (2002) 7193.
[23] A.S.D. Sandanayaka, K. Ikeshita, N. Watanabe, Y. Araki, Y. Furusho, N. Kihara, T. Takata, O. Ito, Bull. Chem. Soc. Jpn 78 (2005) 1008.
[24] F. Mohamadi, N.G.J. Richards, W.C. Guida, R. Liskamp, M. Lipton, C. Gaufield, G. Chang, T. Hendrickson, W.C. Still, J. Comput. Chem. 11 (1990) 440.
[25] O. Ito, Y. Sasaki, Y. Yoshikawa, A. Watanabe, J. Phys. Chem. 99 (1995) 9838.
[26] Y. Yahata, Y. Sasaki, M. Fujitsuka, O. Ito, J. Photosci. 6 (1996) 117.
[27] M. Fujitsuka, O. Ito, T. Yamashiro, Y. Aso, T. Otsubo, J. Phys. Chem. A 104 (2000) 4876.
[28] C. Luo, M. Fujitsuka, A. Watanabe, O. Ito, L. Gan, H. Huang, C.-H. Huang, J. Chem. Soc., Faraday Trans. 94 (1998) 527.
[29] B. Ma, Y.-D. Sun, S.-K. Kim, J. Am. Chem. Soc. 114 (1992) 4429.
[30] D.M. Guldi, M. Prato, Acc. Chem. Res. 33 (2000) 695.
[31] A.S.D. Sandanayaka, Y. Araki, C. Luo, M. Fujitsulka, O. Ito, Bull. Chem. Soc. Jpn 77 (2004) 1313.
[32] K.H. Hausser, J.N. Murrell, J. Chem. Phys. 27 (1957) 500.
[33] G.J. Kavarnos, N.J. Turro, Chem. Rev. 86 (1986) 401.
[34] Y. Sasaki, M. Fujitsuka, A. Watanabe, O. Ito, J. Chem. Soc., Faraday Trans. 93 (1997) 4275.
[35] D.L. Dexter, J. Chem. Phys. 21 (1953) 836.
[36] T. Förster, Naturwissenschaften 33 (1946) 166.